# Micellelike aggregates in solutions of semirigid hairy-rod polymers

Wen-Chung Ou-Yang,[1] Chi-Sheng Chang,[1] Hsin-Lung Chen,[1,*] Cheng-Si Tsao,[2] Kang-Yung Peng,[1] Show-An Chen,[1] and Charles C. Han[3]

[1]*Department of Chemical Engineering, National Tsing Hua University, Hsin-Chu 30013, Taiwan, Republic of China*

[2]*Institute of Nuclear Energy Research, Lungtun, Taoyuan, Taiwan, Republic of China*

[3]*National Institute of Standards and Technology, Gaithersburg, Maryland 20899, USA*

(Received 3 May 2004; revised manuscript received 14 June 2005; published 2 September 2005)

An anomalous aggregation of hairy-rod segments generating nanoscale disklike domains is found to occur in the solution of the semirigid polymer at concentrations well below the threshold lyotropic concentration. These aggregate domains are micellelike in the sense that they exist in equilibrium with a dilute isotropic phase consisting of well dissolved segments. The origin of this aggregation is relevant to the connectivity and amphiphicility of the hairy-rod segments and this process could prevail among semirigid polymers with the disklike domains serving as the nuclei for the development of macroscopic nematic phase as one increases the polymer concentration.

DOI: 10.1103/PhysRevE.72.031802 PACS number(s): 61.25.Hq, 36.20.−r, 61.43.Hv

Liquid crystals constitute a class of soft material whose anisotropic optical, electrical, mechanical, and rheological properties have led to a wide spectrum of practical applications. Many liquid crystalline materials are formed by molecules with the rod geometry. In the solution state, these anisotropic molecules self-organize to form nematic phases above certain threshold concentrations driven by their excluded volume interactions [1,2]. The critical concentration for inducing the lyotropic liquid crystallinity decreases with increasing aspect ratio of the rod molecule.

Lyotropic liquid crystallinity is also accessible for polymers composing of rigid monomer units in the backbone [2,3]. The chains of this type of polymers are usually semirigid represented by successive connection of orientationally correlated or uncorrelated Kuhn segments [4,5]. In the absence of strong segmental attraction, the threshold lyotropic concentration of semirigid polymers is largely determined by the aspect ratio of the Kuhn segment [2].

Many semirigid polymers are constituted by the "hairy-rod segments," where short flexible side chains are bound to the backbone at high density to enhance solubility of the polymers in common organic solvents [6]. As purported by abundant spectroscopic [7–9] and dynamic light scattering studies [10], the solutions of semirigid hairy-rod polymers exhibit one distinct feature in the presence of some sort of aggregates. The physical ground underlying the formation of these aggregates is still an open question. Considering that isotropic-nematic transition is the most common structure transformation along the concentration coordinate predicted by the mean-field theory, it is natural to attribute these aggregates to nematic phase formed by the self-organization of the rod segments. This argument is, however, debatable since the concentration of the solution containing these aggregates can be far below the threshold concentrations prescribed by the aspect ratio of the Kuhn segments [11]. Moreover, the nematic phase appearing above the threshold concentration is characterized by long-range orientational order identifiable under cross-polarized optical microscopy. The aggregates found in dilute semirigid polymer solutions are, however, not observable under optical resolution and may hence be submicron in size.

Using small-angle neutron scattering (SANS), the present study aims at resolving the salient features of the anomalous segmental aggregation in semirigid hairy-rod polymer solutions at large dilution. With the result we attempt to address the effect of connectivity and amphiphicility on the self-organization behavior of rod entity, where a segmental aggregation yielding nanoscale micellelike domains sets in prior to the formal formation of the macroscopic nematic phase.

The semirigid polymer studied here is poly[2-methoxy-5-(2′-ethyl-hexyloxy)-1,4-phenylene vinylene] (MEH-PPV) with the chemical structure displayed in Fig. 1. The number average molecular weight and the polydispersity index of the polymer are 216 000 g/mole and 2.0, respectively. MEH-PPV was dissolved in two deuterated solvents, *d*-chloroform and *d*-toluene, where the former is a good solvent for both the backbone and the side chain whereas the later is a poor and good solvent for the side chain and the backbone, respectively [12]. No sign of macrophase separation was observed in the solutions even after prolonged storage at the room temperature. SANS experiments over the $q$ range from around 0.003 to 0.4 $Å^{-1}$ were carried out using the 30-m SANS instrument at the National Institute of Standards and Technology (NIST) Center for Neutron Research (NCNR). The incoherent backgrounds from the pure solvents were measured, corrected by the volume fraction displaced by the MEH-PPV polymer, and subtracted from the reduced SANS data.

Figure 1 shows the SANS profiles of MEH-PPV/chloroform solutions at 25 °C in a log-log plot. It is noted that the profiles are fairly identical after being normalized by the corresponding polymer concentration in the range of

*Author to whom correspondence should be addressed. Email address: hlchen@che.nthu.edu.tw

 

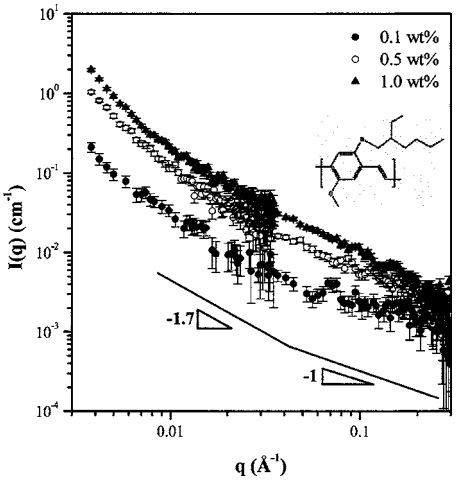


FIG. 1. SANS profiles of MEH-PPV/chloroform solutions at 25 °C in a log-log plot, demonstrating the power law of $I(q)$ in different $q$ regions. The inset shows the chemical structure of MEH-PPV.

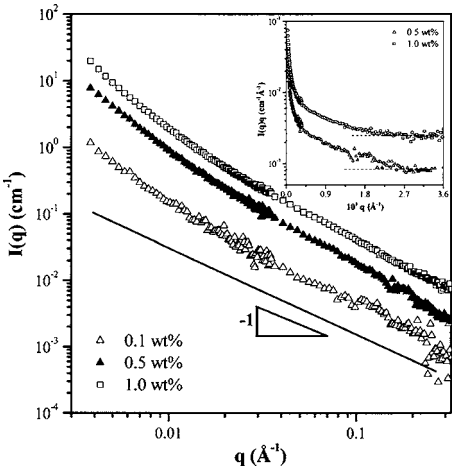


FIG. 2. SANS profiles of MEH-PPV/toluene solutions at 25 °C in a log-log plot. The inset displays the semilog $I(q)q$ plots of 0.5 and 1.0 wt. % solutions, showing a plateau at $q > \sim 0.25$ Å$^{-1}$.

$0.005$ Å$^{-1} < q < 0.4$ Å$^{-1}$; therefore, it is reasonable to consider that the scattering pattern in this $q$ range is associated with the form factor of the molecularly dissolved chains in the relatively good chloroform solvent. The slope in Fig. 1 deviates from around $-1.7$ to around $-1$ at $q \approx 0.04$ Å$^{-1}$ irrespective of the polymer concentration. The power law of $I(q) \sim q^{-1.7}$ in the middle-$q$ region attests that the conformation of MEH-PPV chain is properly described by the expanded linear Gaussian coil under lower spatial resolution [5]. The $q^{-1}$ dependence at high $q$, governed by the local chain structure, corresponds to the rigid rod behavior of the segments constituting the chain [13]. The crossover from the rod to the expanded coil regime ($q_c$) yields an estimate for the length of the Kuhn segment, $b$, *via* $b \approx 7/q_c = 7/0.04$ Å$^{-1} = 175$ Å [14,15]. Considering that the radius of the hairy-rod segment ($R$) is 4.58 Å [16], the aspect ratio of the Kuhn segment is hence $a_r = b/2R \approx 19.1$. This aspect ratio prescribes the threshold lyotropic concentration of around 37.5% according to the semiempirical approximation given by Flory [2,11].

The SANS profiles of MEH-PPV/toluene solutions at 25 °C are displayed in Fig. 2. The transition of the slope from $-1$ to $-1.7$, which was observed from the chloroform solutions, is no longer present. The slope in the high-$q$ region ($0.04$ Å$^{-1} < q < 0.25$ Å$^{-1}$), where the corresponding chloroform solutions display a slope of $-1$ is found to vary with the polymer concentration and is more negative than $-1$ (i.e., $-1.33$, $-1.60$, and $-1.54$ for 0.1, 0.5, 1.0 wt. %, respectively). Furthermore, the toluene solution is found to exhibit a stronger scattered intensity after normalized by the neutron contrast than the chloroform solution of the same concentration (see Fig. 3), which signals aggregation of the rod segments in the former. Consequently, the total coherent scattered intensity from toluene solution is represented by a linear summation of the contributions from the aggregates $I_a(q)$ and the dissolved segments $I_{ds}(q)$. In the high-$q$ region where $I(q)$ is dominated by the form factors of these two components, $I_a(q)$ displays a power law of $I_a(q) \sim q^{-\beta}$ with $\beta > 1$ such that its addition with $I_{ds}(q) \sim q^{-1}$ makes the slope of $I(q)$ $(\sim Aq^{-\beta} + Bq^{-1})$ in log-log plot more negative than $-1$.

A further analysis of the scattering profiles in Fig. 2 reveals that the slope actually recovers the value of around $-1$ in the tail region ($q > 0.25$ Å$^{-1}$), as manifested from the inset in Fig. 2 showing a plateau in the $I(q)q$ vs $q$ plot of 0.5 and 1.0 wt. % solutions in this region. This can be understood by considering that in the high-$q$ region $I_a(q)$ $(\sim q^{-\beta}, \beta > 1)$ falls more rapidly than $I_{ds}(q)$ $(\sim q^{-1})$, such that $I(q)$ becomes dominated by $I_{ds}(q)$ in the tail region. In this case, $I_{ds}(q)$ at high $q$ is given by a line with a slope of $-1$ extended from the tail region. The form factor of the aggregate in this $q$ region can then be unveiled by subtracting $I_{ds}(q)$ thus extrapolated from $I(q)$. Figure 4 displays $I_a(q)$ obtained from the subtraction procedure for 0.5 and 1.0 wt. % solutions. The plots are found to possess a slope of around $-2$, indicating that the aggregates are *disklike* domains [12] in which the rod segments pack laterally leading to orientational order on a nanoscale.

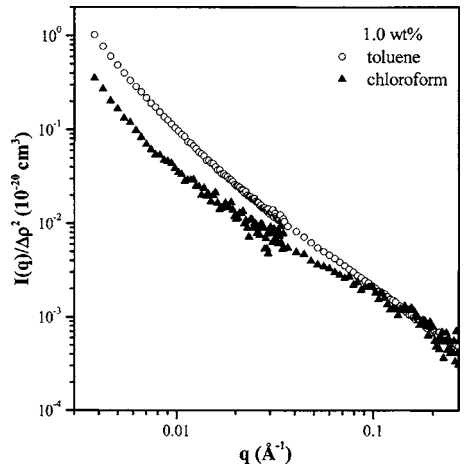


FIG. 3. Neutron contrast-normalized profiles of 1.0 wt. % toluene and chloroform solutions.

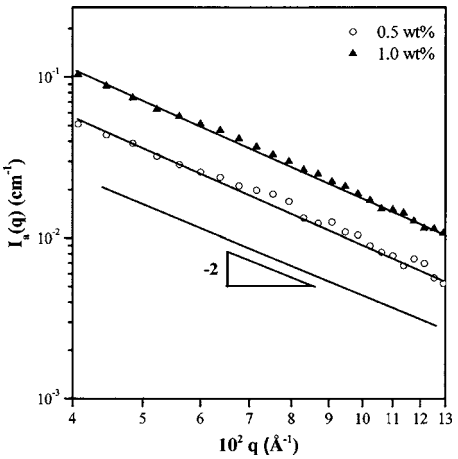


FIG. 4. $I_a(q)$ in a log-log plot obtained from the subtraction procedure for 0.5 and 1.0 wt. % solutions at 25 °C.

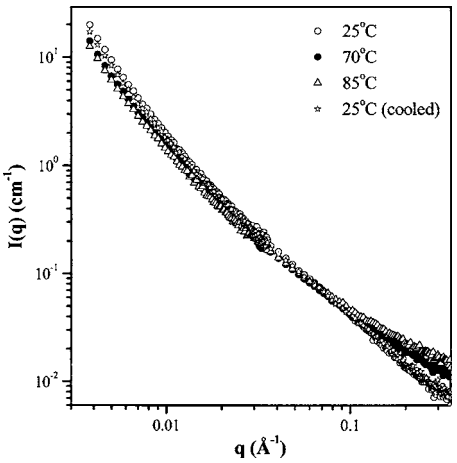


FIG. 5. A series of SANS profiles of 1.0 wt. % toluene solution collected *in situ* in a heating cycle. The SANS profile of the solution cooled from 85 to 25 °C after the heating experiment is also displayed to demonstrate the good thermal reversibility of the segmental aggregation.

Temperature-dependent SANS experiments were conducted to gain further insight into the structure of the dislike aggregates. Figure 5 displays a series of SANS profiles of 1.0 wt. % toluene solution collected *in situ* in a heating cycle. The temperature dependence of the scattering profile is characterized by a systematic decrease and increase in the scattered intensity at low/middle $q$ ($q<0.03$ Å$^{-1}$) and high $q$ ($q>0.08$ Å$^{-1}$), respectively, with increasing temperature. The slope in the high-$q$ region also approaches $-1$ with increasing temperature. The decrease in the low-$q$ intensity asserts that the aggregate concentration decreases with increasing temperature and such a deaggregation increases the concentration of the dissolved segments and hence enhances the high-$q$ intensity contributed by the form factor of this species.

A cooling experiment was performed right after the heating cycle to explore the thermal reversibility of the segmental aggregation. The intensity curve collected at a specific temperature (i.e., 70 and 25 °C) in the cooling cycle is found to be virtually identical to that obtained at the same temperature in the heating cycle (see the scattering curve of 25 °C in Fig. 5), showing that the reaggregation upon cooling proceeds rapidly without involving large nucleation barrier. Moreover, the fact that the aggregate concentration at a given temperature is virtually identical in the heating and cooling cycles strongly implies that the aggregates are in equilibrium with a dilute isotropic phase consisting of well-dissolved segments, which is reminiscent of the equilibrium between micelles and unimers in the solution of amphiphilic molecules. It should be noted that the nanoscale aggregation observed is not described straightforwardly by the framework of the classical theories of lyotropic liquid crystallinity in the sense that the micellelike aggregates develop at the concentration far lower than the threshold lyotropic concentration (around 37.5 %) estimated from the mean-field theory.

The connectivity and amphiphicility of the hairy-rod segments may be responsible for the anomalous segmental aggregation. Since the overlap concentration of the polymer chains in solution is inversely proportional to the third power of the average end-to-end distance of the chains [17], semirigid chains (having large end-to-end distance due to chain stiffness) may overlap with one another easily at low concentration (say, less than 0.1 wt. %). A consequence of the interchain overlap is enrichment of segments around the overlap points, where the segmental concentration around these regions is higher than the average concentration. In other words, the connectivity of the rod segments along the chains forces a fraction of them to meet around the overlap points. The convention of these segments may be transient since random Brownian force tends to drive them apart; therefore, an attractive force between the hairy-rod segments is necessary to stabilize their aggregation around the overlap points. Such an attractive force is offered by the amphiphicility of the hairy-rod segments [18–21], where in the present case the poor affinity of the side chains to toluene solvent produces a segmental attraction.

In conclusion, we have shown that the hairy-rod segments of MEH-PPV conjugated polymer formed disklike aggregates with micellelike character in toluene at large dilution. This anomalous aggregation may be driven by the connectivity and amphiphicility of the rod segments. It is also worth noting that the nanoscale segmental aggregation observed here could prevail among various types of semirigid polymers and the disklike domains thus generated may serve as the nuclei for promoting the development of macroscopic nematic phase as one increases the polymer concentration.

We gratefully acknowledge financial support from the Ministry of Education under Contract No. 91E-FA04-2-4A. The supports of NIST, U.S. Department of Commerce, and the National Science Foundation, through Agreement No. DMR-9986442, in providing the neutron research facilities used in this work are gratefully acknowledged. Thanks are also due to Dr. Derek L. Ho at NIST for assistance in SANS experiment and helpful discussions, and to Professor An-Chung Su at the National Sun Yat-sen University for useful comments.

[1] L. Onsager, Ann. N.Y. Acad. Sci. **51**, 627 (1949).
[2] P. J. Flory, Adv. Polym. Sci. **59**, 1 (1984).
[3] T. Itou and A. Teramoto, Macromolecules **21**, 2225 (1988).
[4] A. R. Khokhlov and A. N. Semenov, Physica A **108A**, 546 (1981).
[5] M. Rubinstein and R. H. Colby, *Polymer Physics* (Oxford University, Oxford, 2003).
[6] R. Stepanyan *et al.*, Macromolecules **36**, 3758 (2003).
[7] T.-Q. Nguyen, V. Doan, and B. J. Schwartz, J. Chem. Phys. **110**, 4068 (1999).
[8] C. J. Collison, L. J. Rotherberg, V. Treemaneekarn, and Y. Li, Macromolecules **34**, 2346 (2001).
[9] J.-H. Hsu *et al.*, J. Phys. Chem. A **103**, 2375 (1999).
[10] G. Petekidis *et al.*, Macromolecules **30**, 919 (1997).
[11] The threshold lyotropic concentration of semirigid polymer solutions can be estimated by the semiempirical equation $\phi_p^* = (8/a_r)(1-2/a_r)$ with $a_r$ being the aspect ratio of the Kuhn segment (Ref. [2]). $\phi_p^*$ normally lies above 10% except for some systems constituted by Kuhn segments with very large aspect ratio ($>80$).
[12] Y. Shi, J. Liu, and Y. Yang, J. Appl. Phys. **87**, 4254 (2000).
[13] R.-J. Roe, *Methods of X-ray and Neutron Scattering in Polymer Science* (Oxford University, New York, 2000).
[14] J. Des Cloizoaux, Macromolecules **6**, 403 (1973).
[15] T. Yoshizaki and H. Yamakawa, Macromolecules **13**, 1518 (1980).
[16] $R$ was obtained from the mass per unit length ($M_L$) of the rod segment via $R=(M_L/\pi\rho_m)^{1/2}=4.58$ Å using $M_L=6.45\times10^{-15}$ g/cm (calculated from the monomer length of 6.7 Å) (Ref. [22]) and $\rho_m=0.98$ g/cm$^3$ (the mass density of MEH-PPV).
[17] G. R. Strobl, *The Physics of Polymers* (Springer-Verlag, Berlin, 1996).
[18] S. H. Chen, C. H. Su, A. C. Su, and S. A. Chen, J. Phys. Chem. B **108**, 8855 (2004).
[19] M. Prehm *et al.*, J. Am. Chem. Soc. **124**, 12 072 (2002).
[20] M. Sone *et al.*, Macromolecules **31**, 8865 (1998).
[21] S. H. Chen *et al.*, Macromolecules **37**, 181 (2004).
[22] S. H. Chen *et al.*, Macromolecules **35**, 4229 (2002).